Spectral morphological analysis of skin lesions with a polarization multispectral dermoscope

Dimitrios Kapsokalyvas,[1,*] Nicola Bruscino,[2] Domenico Alfieri,[3] Vincenzo de Giorgi,[2] Giovanni Cannarozzo,[2] Riccardo Cicchi,[4,1] Daniela Massi,[5] Nicola Pimpinelli,[2] and Francesco S. Pavone[1,4,6]

[1]*European Laboratory for Non-linear Spectroscopy (LENS), Univ. of Florence, 50019, Sesto-Fiorentino, Italy*
[2]*Division of Clinical, Preventive and Oncology Dermatology, Department of Critical Care Medicine and Surgery, University of Florence, 50129, Florence, Italy*
[3]*Light4tech Firenze Srl, 50018, Scandicci, Italy*
[4]*National Institute of Optics, National Research Council, Largo 50125, Florence, Italy*
[5]*Division of Human Pathology and Oncology, Department of Critical Care Medicine and Surgery, University of Florence, 50134, Florence, Italy*
[6]*Department of Physics and Astronomy, University of Florence, Sesto Fiorentino,50019, Italy*
**kapsokalyvas@lens.unifi.it*

Abstract: Dermoscopy is the conventional technique used for the clinical inspection of human skin lesions. However, the identification of diagnostically relevant morphologies can become a complex task. We report on the development of a polarization multispectral dermoscope for the *in vivo* imaging of skin lesions. Linearly polarized illumination at three distinct spectral regions (470, 530 and 625 nm), is performed by high luminance LEDs. Processing of the acquired images, by means of spectral and polarization filtering, produces new contrast images, each one specific for melanin absorption, hemoglobin absorption, and single scattering. Analysis of such images could facilitate the identification of pathological morphologies.

OCIS codes: (170.6510) Spectroscopy, tissue diagnostics; (170.1870) Dermatology; (110.2945) Illumination design; (100.2980) Image enhancement.

References and links

1. I. Zalaudek, G. Argenziano, A. Di Stefani, G. Ferrara, A. A. Marghoob, R. Hofmann-Wellenhof, H. P. Soyer, R. Braun, and H. Kerl, "Dermoscopy in general dermatology," Dermatology (Basel) **212**(1), 7–18 (2006).
2. R. P. Braun, H. S. Rabinovitz, M. Oliviero, A. W. Kopf, and J. H. Saurat, "Dermoscopy of pigmented skin lesions," J. Am. Acad. Dermatol. **52**(1), 109–121 (2005).
3. S. Menzies, *Dermoscopy: An Atlas* (McGraw-Hill, Sydney, 2009).
4. A. A. Marghoob, R. P. Braun, and A. W. Kopf, *Atlas of Dermoscopy* (Taylor & Francis, London; New York, 2005).
5. J. Malvehy, *Handbook of Dermoscopy* (Taylor & Francis, London, 2006).
6. F. Nachbar, W. Stolz, T. Merkle, A. B. Cognetta, T. Vogt, M. Landthaler, P. Bilek, O. Braun-Falco, and G. Plewig, "The ABCD rule of dermatoscopy. High prospective value in the diagnosis of doubtful melanocytic skin lesions," J. Am. Acad. Dermatol. **30**(4), 551–559 (1994).
7. G. Argenziano, G. Fabbrocini, P. Carli, V. De Giorgi, E. Sammarco, and M. Delfino, "Epiluminescence microscopy for the diagnosis of doubtful melanocytic skin lesions. Comparison of the ABCD rule of dermatoscopy and a new 7-point checklist based on pattern analysis," Arch. Dermatol. **134**(12), 1563–1570 (1998).
8. H. Pehamberger, A. Steiner, and K. Wolff, "In vivo epiluminescence microscopy of pigmented skin lesions. I. Pattern analysis of pigmented skin lesions," J. Am. Acad. Dermatol. **17**(4), 571–583 (1987).
9. S. W. Menzies, C. Ingvar, and W. H. McCarthy, "A sensitivity and specificity analysis of the surface microscopy features of invasive melanoma," Melanoma Res. **6**(1), 55–62 (1996).
10. Derma Medical Systems Handels und Entwicklungs GmbH, "Mole Max," (2012), *http://www.dermamedicalsystems.com*.
11. M. Moncrieff, S. Cotton, E. Claridge, and P. Hall, "Spectrophotometric intracutaneous analysis: a new technique for imaging pigmented skin lesions," Br. J. Dermatol. **146**(3), 448–457 (2002).

#175601 - $15.00 USD Received 14 Sep 2012; revised 10 Dec 2012; accepted 7 Jan 2013; published 20 Feb 2013

12. S. W. Menzies, L. Bischof, H. Talbot, A. Gutenev, M. Avramidis, L. Wong, S. K. Lo, G. Mackellar, V. Skladnev, W. McCarthy, J. Kelly, B. Cranney, P. Lye, H. Rabinovitz, M. Oliviero, A. Blum, A. Varol, B. De'Ambrosis, R. McCleod, H. Koga, C. Grin, R. Braun, and R. Johr, "The performance of SolarScan: an automated dermoscopy image analysis instrument for the diagnosis of primary melanoma," Arch. Dermatol. **141**(11), 1388–1396 (2005).
13. M. Elbaum, A. W. Kopf, H. S. Rabinovitz, R. G. Langley, H. Kamino, M. C. Mihm, Jr., A. J. Sober, G. L. Peck, A. Bogdan, D. Gutkowicz-Krusin, M. Greenebaum, S. Keem, M. Oliviero, and S. Wang, "Automatic differentiation of melanoma from melanocytic nevi with multispectral digital dermoscopy: a feasibility study," J. Am. Acad. Dermatol. **44**(2), 207–218 (2001).
14. R. R. Anderson and J. A. Parrish, "The optics of human skin," J. Invest. Dermatol. **77**(1), 13–19 (1981).
15. G. Zonios, J. Bykowski, and N. Kollias, "Skin melanin, hemoglobin, and light scattering properties can be quantitatively assessed in vivo using diffuse reflectance spectroscopy," J. Invest. Dermatol. **117**(6), 1452–1457 (2001).
16. S. H. Tseng, P. Bargo, A. Durkin, and N. Kollias, "Chromophore concentrations, absorption and scattering properties of human skin in-vivo," Opt. Express **17**(17), 14599–14617 (2009).
17. S. G. Demos and R. R. Alfano, "Optical polarization imaging," Appl. Opt. **36**(1), 150–155 (1997).
18. V. Sankaran, J. T. Walsh, Jr., and D. J. Maitland, "Comparative study of polarized light propagation in biologic tissues," J. Biomed. Opt. **7**(3), 300–306 (2002).
19. S. L. Jacques, J. R. Roman, and K. Lee, "Imaging superficial tissues with polarized light," Lasers Surg. Med. **26**(2), 119–129 (2000).
20. R. R. Anderson, "Polarized light examination and photography of the skin," Arch. Dermatol. **127**(7), 1000–1005 (1991).
21. S. A. Prahl and S. L. Jacques, "Optical properties spectra" (2001), *http://omlc.ogi.edu/spectra/*.
22. S. L. Jacques, J. C. Ramella-Roman, and K. Lee, "Imaging skin pathology with polarized light," J. Biomed. Opt. **7**(3), 329–340 (2002).
23. G. Zonios, A. Dimou, I. Bassukas, D. Galaris, A. Tsolakidis, and E. Kaxiras, "Melanin absorption spectroscopy: new method for noninvasive skin investigation and melanoma detection," J. Biomed. Opt. **13**(1), 014017 (2008).
24. S. Demos, H. Radousky, and R. Alfano, "Deep subsurface imaging in tissues using spectral and polarization filtering," Opt. Express **7**(1), 23–28 (2000).
25. J. O'Doherty, J. Henricson, C. Anderson, M. J. Leahy, G. E. Nilsson, and F. Sjöberg, "Sub-epidermal imaging using polarized light spectroscopy for assessment of skin microcirculation," Skin Res. Technol. **13**(4), 472–484 (2007).
26. Y. Bae, J. S. Nelson, and B. Jung, "Multimodal facial color imaging modality for objective analysis of skin lesions," J. Biomed. Opt. **13**(6), 064007 (2008).
27. W. A. Bruls and J. C. van der Leun, "Forward scattering properties of human epidermal layers," Photochem. Photobiol. **40**(2), 231–242 (1984).
28. J. R. Mourant, M. Canpolat, C. Brocker, O. Esponda-Ramos, T. M. Johnson, A. Matanock, K. Stetter, and J. P. Freyer, "Light scattering from cells: the contribution of the nucleus and the effects of proliferative status," J. Biomed. Opt. **5**(2), 131–137 (2000).
29. M. Rajadhyaksha, M. Grossman, D. Esterowitz, R. H. Webb, and R. R. Anderson, "In vivo confocal scanning laser microscopy of human skin: melanin provides strong contrast," J. Invest. Dermatol. **104**(6), 946–952 (1995).
30. S. Q. Wang, S. W. Dusza, A. Scope, R. P. Braun, A. W. Kopf, and A. A. Marghoob, "Differences in dermoscopic images from nonpolarized dermoscope and polarized dermoscope influence the diagnostic accuracy and confidence level: a pilot study," Dermatol. Surg. **34**(10), 1389–1395 (2008).
31. G. Argenziano, I. Zalaudek, R. Corona, F. Sera, L. Cicale, G. Petrillo, E. Ruocco, R. Hofmann-Wellenhof, and H. P. Soyer, "Vascular structures in skin tumors: a dermoscopy study," Arch. Dermatol. **140**(12), 1485–1489 (2004).

1. Introduction

Dermoscopy (dermatoscopy, epiluminescence microscopy, surface microscopy) is a potent but at the same time very simple technique used for clinical visual inspection of a skin lesion [1–5]. The dermoscope is a hand held device consisting of a magnifying lens and a white light source. Liquid medium, usually immersion oil, is applied between the instrument and the skin, to eliminate surface reflection. The observation is performed by the eye of a trained dermatologist and often a digital camera is attached for image recording. This technique is usually used for determining whether a lesion is benign or malignant and pathologies such as Melanoma, Basal Cell Carcinoma (BCC), Seborrheic Keratosis, vascular lesions and Dermatofibroma can be diagnosed [3–5]. Especially for the case of pigmented lesions, several diagnostic methodologies have been developed based on the morphological characteristics revealed by dermoscopic images. The ABCD rule [6] and the 7-point check list [7] assign a score to the pigmented lesion according to its morphological features based on which

#175601 - $15.00 USD Received 14 Sep 2012; revised 10 Dec 2012; accepted 7 Jan 2013; published 20 Feb 2013

diagnosis is made. Pattern analysis [8] and the Menzies method [9] correlate the presence of specific patterns with malignancy. These methodologies improve the diagnostic accuracy of dermoscopy when they are performed by a well trained expert. Nevertheless, a large number of equivocal lesions found in the clinical examination are diagnosed with the so called "gold standard" method, which requires biopsy or surgery followed by histopathological examination.

In addition to avoiding an unnecessary excision of a lesion for biopsy, which is a costly and time consuming method, the need for higher sensitivity and specificity has led to the development of techniques and devices that can offer additional information. Some of these approaches have resulted in commercial implementations such as MoleMax [10], SIAscope [11], SolarScan [12], and MelaFind [13]. These instruments are essentially dermoscopes, and operate in a similar manner. A common feature is the use of state of the art camera systems and additional image analysis software for better documentation and follow-up of the cases. Furthermore, SIAscope and Melafind use several different wavelengths for illumination, and elaborate computer algorithms for revealing morphological characteristics of the lesions. MoleMax uses polarized light for illumination, and software for automatic classification. SolarScan employs an RGB camera to produce images of the reflectivity of a lesion, and follows its evolution in time. Nevertheless, none of these approaches targets on enhancing the contrast of structures and morphologies which have low visibility in the dermoscopic image, but could be important for the diagnosis.

This study aims at developing a device that has all the advantages of a dermoscope, but can offer additional features useful for diagnosis. To do so, the optical properties of skin were taken into consideration in order to design the device. The absorption properties of skin *in vivo* in the visible spectrum are characterized by the absorption of melanin and hemoglobin [14–16]. It is possible to enhance the intensity contrast of these chromophores in the image by selecting an illumination spectrum close to their absorption maxima. Additionally, light backscattered from deeper layers of the skin is depolarized [17–19]. It has been demonstrated that viewing skin lesions under linearly polarized illumination enhances the surface details when detecting through a parallel polarizer, or deep features such as vasculature and pigmentation when detecting through a cross polarizer [20].

A conventional dermoscope records the image of the diffuse reflection of white light from the skin. The implementation reported here employs high luminance LEDs for the illumination at three distinct spectral regions (blue, green and red), a polarizer for illumination, and a rotating analyzer for detection. LEDs were selected as the illumination source because they can provide the desired wavelengths, are inexpensive, and practical. Image-processing of multispectral polarization images allowed us to produce images specific for blood vessel morphology, melanin localization, and scattering structures. The novelty of our approach lies in the fact that the images produced are specific for each major skin component thus facilitating the morphology identification. The device was used to examine several pathologic lesions. Here two relevant cases are presented in order to demonstrate the proof of principle and the methodology of this approach.

2. Materials and methods

2.1 Experimental setup

The Polarization Multispectral Dermoscope consists of four parts. The dermoscope head, the tripod on which the head is mounted, the electronics control box, and the computer where the images are stored and processed (Fig. 1(b)). It can be used with the aid of the tripod, which increases the stability, or it can be hand held, especially for imaging body sites where access is difficult.

The dermoscope head (Fig. 1(a)) houses the lens, the LEDs, the polarizer, the analyzer, and the camera. For the illumination, twelve high luminance Luxeon Star/O LEDs (Philips

#175601 - $15.00 USD Received 14 Sep 2012; revised 10 Dec 2012; accepted 7 Jan 2013; published 20 Feb 2013

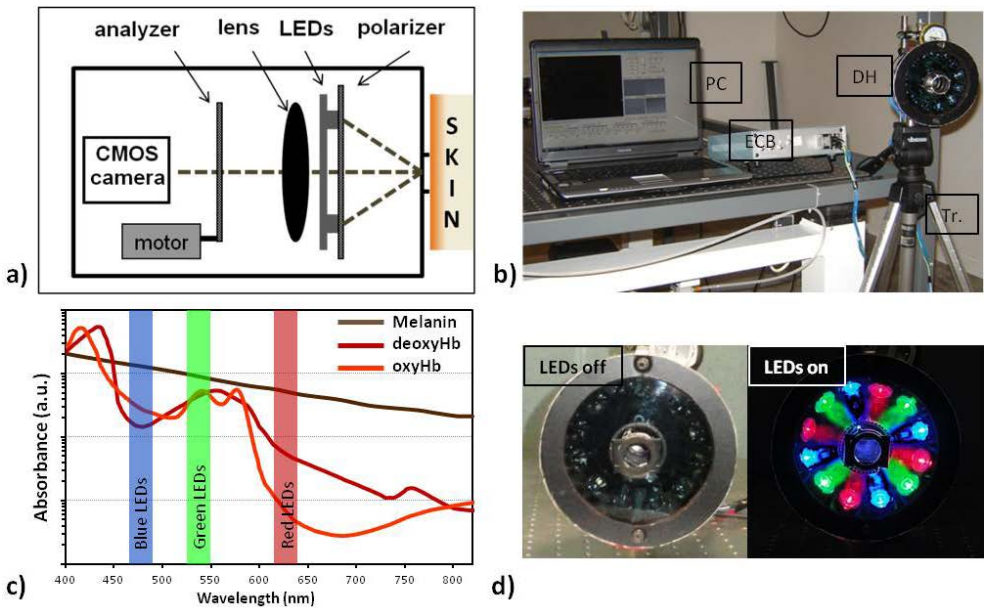

Fig. 1. a) Diagram of the Dermoscope head b) Image of the Polarization Multispectral Dermoscope where the main parts of the device can be seen, DH: dermoscope head, the circular arrangement of the LEDS can be seen and the polarizer is placed in front the LEDs, ECB: electronics control box, PC: the computer used for instrument control and image acquisition, Tr. A tripod used to mount the device. c) Absorption spectrum of Hemoglobin (oxyHb: oxygenated Hemoglobin, deoxyHb: deoxygenated Hemoglobin) and Melanin (reproduced from Ref. [21]). The graph is in logarithmic scale in arbitrary units of absorbance. The illumination spectrum of each LED set according to their FWHM is indicated on the graph. d) front view of the dermoscope head with LEDs off and on.

Lumileds Lighting Company, San Jose, CA, USA) of 1 Watt power consumption are used. Four of them emit at 470 nm (Blue) with Full Width at Half Maximum (FWHM) of 25 nm, another four emit at 530 nm (Green) with FWHM of 35 nm, and the last four emit at 625 nm (Red) with FWHM of 20 nm (Fig. 1(c)). The LEDs employ a batwing profile lens for reducing the illumination to a viewing angle of 10°. Each type of LED is positioned symmetrically on the periphery of a circle, as seen in Fig. 1(d), and they are bent at a 45° angle in order to illuminate homogeneously the skin lesion. The homogeneity of the illumination is tested by taking an image of the reflection from white photographic paper, and is considered acceptable when the standard deviation of the image's intensity is less than 3% of the mean intensity. This adjustment is performed for each LED set separately. A ring-shaped polarizing plate is mounted in front of the LEDs for polarizing the illumination. This polarizing plate (CCS Inc., Japan) is circular (120 mm) with a hollow center (40 mm) allowing the reflected light to pass through. The skin lesion is positioned on a glass window and is optically coupled to the skin by a drop of water. The glass window is held by a spacer. On top of the glass there is an O-ring which marks and stabilizes the position of the skin lesion. The lens (achromatic doublet, f = 30mm) which focuses the reflected light to the CMOS camera is positioned at an equal distance between the skin lesion and the camera, and the magnification is 1. The analyzer (CCS Inc., Japan) is placed in front of the camera and is mounted on a motorized rotator. The motor is configured to rotate the analyzer to two positions; one is 0° and the other is 90° with respect to the polarizer, which from now on will be called position 0 and position 90. The CMOS color camera (uEye, UI-1440-C, IDS Imaging Development Systems GmbH, Obersulm, Germany) is connected to a laptop PC via USB and has 1280 × 1024 pixel resolution. The field of view on the skin lesion is 8 mm × 6.4 mm. The images are stored in the PC, and subsequently processed with ImageJ (NIH,

#175601 - $15.00 USD Received 14 Sep 2012; revised 10 Dec 2012; accepted 7 Jan 2013; published 20 Feb 2013

Bethesda, Maryland, USA). The switches and the power supply for the LEDs and the motor are housed in a custom made electronics control box.

2.2. Image acquisition

When a lesion is examined five images are acquired. Before the acquisition, the exposure time of the camera is adjusted differently for each LED's color set in order to achieve similar intensities on a region of the skin which is outside the lesion, a perilesional region. First the analyzer is set at the 0 position (analyzer parallel to polarizer). The lesion is illuminated with the blue LEDs and the *Blue0* image is recorded. Then the analyzer is set at position 90 (analyzer perpendicular to polarizer). Illumination with each LED set separately yields the *Blue90, Green90,* and *Red90* images. Simultaneous illumination with all the LEDs creates white light illumination on the skin lesion. The gain for each color is adjusted by the camera software in order to have a good white balance, and the *White90* image is recorded. This image is the equivalent of an image acquired with a conventional modern dermoscope. It offers a general view of the lesion, and from now on will be called the dermoscopic image. The images acquired are RGB 24-bit color images and are stored in bitmap file format (.bmp). These images are subsequently processed in order to extract additional information, not visible in the dermoscopic image.

In classical dermoscopy lesions with very different absorption characteristics are imaged. In order to produce bright enough images for each case, either the illumination intensity or the exposure time of the camera is adjusted. Similar to classical dermoscopy we chose to adjust the exposure time of our sensor. However, since we perform illumination at three different spectral regions we need to equalize those images. Our method of equalization is to adjust the exposure time of the camera in order to produce the same intensity level in a perilesional region for the Blue90, Green90 and Red90 images. It is recommended to adjust this level at the middle of the dynamic range. In melanocytic lesions this level can be adjusted to slightly higher values in cases where absorption is very high and imaging results in intensities below the noise level. Therefore changes inside the lesion are assigned to variation of the concentration of chromophores and scattering structures. With targeted image processing these changes can be contrast enhanced. There are limitations in our methodology and those occur when heavily pigmented lesions are imaged. In these cases, due to very high absorption from melanin, our processing methods are not followed as they are prone to artifacts. The reliability of the methods is not yet quantified and a larger number of cases is needed to asses this. However, the method is considered valid as long as the images acquired are not saturated nor have intensity levels below the noise level.

2.3. Volunteers

The device was employed for imaging skin lesions on volunteers in the Dermatology Clinic of the University of Florence. The study was approved by the Institutional Review Board of the University of Florence, and conducted according to the tenets of the Declaration of Helsinki. Written informed consent was obtained from all study participants after detailed explanation of the study. The volunteers were selected randomly among the individuals who visited the clinic.

The case presented in Fig. 2 is from the right shoulder of a 41 year old male. The clinical and histological diagnosis for this case was Basal Cell Carcinoma. The case presented in Fig. 3 is from the dorsal forearm of a 25 year old female. The clinical diagnosis for this case was melanocytic nevus.

2.4 Image processing

For performing the processing algorithms described in the text below, the RGB channels (Red, Green, Blue) of each spectral image are summed in one image, and any successive operation is performed on this image. All the operations are performed pixel by pixel. At the

#175601 - $15.00 USD Received 14 Sep 2012; revised 10 Dec 2012; accepted 7 Jan 2013; published 20 Feb 2013

end of the algebraic manipulations the resulting image is converted to 8-bit gray scale image, by assigning the 0 to the minimum value and 255 to the maximum, and saved in bitmap format. This is a common file format and the images can be displayed on any computer system.

There are three types of processing algorithms performed with the acquired images: Scattering Contrast, Blood Contrast and Melanin Contrast. An ImageJ plug-in, which automatically performs the processing of the images immediately after the acquisition and displays the results, has been created.

A simplified model to interpret the intensity of the recorded images is used. We assume that the major chromophores in the skin are melanin and hemoglobin [14–16]. We assume that the light detected is back-scattered from the skin. The images acquired in the 0 position are images which contain the contribution of single scattered photons and deeply penetrating multiple scattered photons, whereas the images acquired in the 90 position are images containing only the contribution of the deeper penetrating multiple scattered photons [20, 22]. When acquiring the images, the criterion for the exposure time of the camera is to produce images with similar perilesional intensities. In this way, in the perilesional region the intensity of the Blue90, Green90 and Red90 images is equivalent, and inside the lesion the change of the recorded intensity depends on the variation of the concentration of melanin and hemoglobin and the presence of scattering structures. Therefore, it is possible to normalize these three images according to their intensity in the perilesional region and then by image processing perform a targeted contrast enhancement for the various optical components inside the lesion.

3. Results

The processing algorithms to be applied depend on the nature of the lesion. Similar to classical dermoscopy, we divide the analysis of the images in two categories: **Melanocytic** and **Non-melanocytic**. This is required because different morphologies can be imaged in each case, and a different set of processing algorithms is applied. The components of the skin which are highlighted are the same in both cases (melanin, hemoglobin and single scattering), however, the intermediate steps to achieve these results can differentiate. Below, the developed algorithms are described and justified.

3.1 Non-melanocytic lesions

When a lesion is classified as non-melanocytic, a set of processing algorithms is applied to enhance the morphological features that may exist. The algorithms applied are Melanin Contrast, Blood Contrast and Scattering Contrast.

3.1.1. Melanin contrast

Melanin is a natural pigment normally found in the epidermis of the skin, and produced by the melanocytes. It is inserted in membranous particles called melanosomes which are subsequently transferred to other cells of the epidermis. Small scale melanocytic structures may be found in non-melanocytic lesions, which in many cases can be correlated to specific pathologies [3–5]. The aim of the Melanin Contrast method is to produce an image specific for these pigmented structures, and present them in a separate image where they have higher contrast, and the obscurity from other structures is eliminated. The melanin absorption spectrum is broad with a characteristic exponential decay towards longer wavelengths (Fig. 1(c)) [14, 15, 23]. The other dominant pigment in skin, hemoglobin, has a characteristic absorption band in the green spectral region (~550 nm) and absorption is reduced significantly in the 625 nm spectral region which is the illumination wavelength for the Red90 image (Fig. 1(c)). Blood vessels are invisible in the Red90 image, and for this reason this image is used to produce an enhanced contrast image for melanocytic structures. The intensity of the RGB channels ($Red90^{red}$, $Red90^{green}$, $Red90^{blue}$) of the image are summed in

#175601 - $15.00 USD Received 14 Sep 2012; revised 10 Dec 2012; accepted 7 Jan 2013; published 20 Feb 2013

one channel ($Red90^{1ch} = Red90^{red} + Red90^{green} + Red90^{blue}$), and afterwards the range of the image is defined by assigning the 0 value to the minimum value ($\min(Red90^{1ch})$) and the 255 value to the maximum value ($\max(Red90^{1ch})$). Therefore, the colored Red90 image is converted to an 8-bit gray-scale image, using Eq. (1), where the dynamic range of the image is maximized, and as a result pigmented structures appear with increased contrast. Since these melanocytic structures are absorbing structures they are encoded with dark grey values:

$$\text{Melanin Contrast} = \frac{Red90^{1ch} - \min\left(Red90^{1ch}\right)}{\max\left(Red90^{1ch}\right) - \min\left(Red90^{1ch}\right)} \bullet 255 \quad (1)$$

The result can be observed in Fig. 2 on a case of Basal Cell Carcinoma (BCC). In the dermoscopic image (Fig. 2(a)), which is the equivalent of an image recorded with a conventional dermoscope, several absorbing structures are visible. The main characteristic is the presence of blood vessels and small scale melanocytic structures. In the Red90 (Fig. 2(c)) contrast comes mainly from melanin absorption, and the blood vessels are not visible anymore. In the processed image Melanin Contrast (Fig. 2(e)) these small scale melanocytic structures appear with higher contrast. Several pigmented structures can be identified in Fig. 2(e), which correlate to the pathology of BCC, such as the 'spoke wheel area' (arrow), 'peppering' (star) morphology, and 'large ovoid nests' (arrowhead). Histologically, these structures correspond to nests of proliferating pigmented basal cells [5]. Some of these structures can be also observed in the dermoscopic image (Fig. 2(a)), however, in the Melanin Contrast result these morphologies appear with greater contrast, and, most importantly, this image is specific for pigmentation, therefore identification of these structures can be performed with higher specificity.

3.1.2 Blood contrast

The aim of the Blood Contrast method is to enhance the contrast of hemoglobin absorption. The subtraction of spectral images in order to reveal the presence or enhance the contrast of scattering [24] absorbing [25], and fluorescent [26] subjects has been reported. We employ a similar technique by performing the subtraction of the Red90 image from the Green90. Hemoglobin is found in the blood vessels, which are located in the dermis and hypodermis. Hemoglobin can be found in two forms: the oxy-hemoglobin (oxyHb), and the deoxy-hemoglobin (deoxyHb), which have slightly different absorption spectra (Fig. 1(c)). The hemoglobin absorption spectrum exhibits a major peak at around 430 nm, and a minor one at around 550 nm [14, 15], which is close to the illumination maximum of the green LEDs used for the Green90 image. Melanin has an absorption spectrum which is characterized by an exponential decay towards longer wavelengths. While the absorption of melanin in the Red90 is about two times smaller compared to the Green90, the corresponding decrease in hemoglobin absorption is almost two orders of magnitude [14, 15] (Fig. 1(c)). Consequently, the effect of hemoglobin absorption is greater in the Green90 image compared to the Red90. By subtracting the Red90 image from the Green90 it is possible to subtract the effect of melanin absorption while maintaining the effect of hemoglobin absorption. Therefore, an image with enhanced contrast for hemoglobin is created by performing the operation in Eq. (2). This is an image that depends on the change of concentration of hemoglobin and thus creates a map of the blood vessels inside the penetration volume of light. As a result, the presence of blood vessels and their morphology in the papillary dermis of skin lesions is revealed. The denominator in Eq. (2) serves as normalization for any inhomogeneity in the illumination. The result of Eq. (2) is converted to an 8-bit image similarly to the method of Eq. (1):

$$\text{Blood Contrast} = \frac{Green90 - Red90}{Green90 + Red90} \quad (2)$$

#175601 - $15.00 USD Received 14 Sep 2012; revised 10 Dec 2012; accepted 7 Jan 2013; published 20 Feb 2013

The result of the Blood Contrast of a case of BCC is illustrated in Fig. 2. The Green90 image (Fig. 2(b)) has high contrast for the vasculature of the lesion as expected, whereas blood vessels are invisible in the Red90 (Fig. 2(c)) image. However, pigmentation is visible in both images. In the Blood Contrast image (Fig. 2(d)) pigmentation morphologies are eliminated, and blood vessel morphology appears with high contrast. A morphology called "arborizing vessels", which describes the treelike terminal branching of blood vessels, is identified in Fig. 2(d) (arrow). This is a characteristic feature of BCC. In this case the big arborizing vessels are also visible in the Green90 image, but in the Blood Contrast image (star), small scale blood vessels invisible in the Green90 image (star in Fig. 2(b)) or in the dermoscopic image (Fig. 2(a)) become visible. Such an image (Fig. 2(d)) can facilitate the identification of pathologic blood vessel morphologies.

3.1.3 Scattering contrast

The aim of the Scattering Contrast method is to enhance the contrast of single scattered photons. When light is directed to the skin, part of the incident light is first reflected on the surface of the skin, the stratum corneum. Scattering inside the epidermis is mainly in the forward direction [27]. A fraction of light can be back-scattered by cell membranes, cell organelles [28], densely-packed keratin fibers, and melanosomes, especially when their concentration exceeds the normal values, as in the case of a nevus or a melanoma [29]. Below the epidermis lies the dermis which is constituted mainly of a dense network of collagen fibers. Collagen is birefringent and a potent scatterer. Light inside the dermis is scattered multiple times, and it is either propagated to an adjacent skin layer, or absorbed [19].

In the case of linearly polarized illumination, light back-scattered from the skin can be divided in two components: one polarized and one depolarized [17, 19, 22]. The polarized fraction retains the initial polarization of the illumination, and it is the fraction that has been single scattered. The other component, the depolarized one, is constituted of photons that have penetrated deeper into the skin, in the dermal layer; they have interacted with the birefringent collagen, and have been multiply scattered. Collagen fibers can assume all possible orientations, and the net effect of birefringence and scattering on polarized light will be the random rotation of polarization [19]. As a consequence, the depolarized component will have equal contribution in all polarization angles, and therefore half can be detected in the 0 position and the other half in the 90. As a result, the images acquired in the 0 position are constructed by single scattered photons, and half of the multiple scattered photons and the images acquired in the 90 position are constructed by the other half of the multiple scattered photons [22].

There are several examples in literature of how to separate these two components of skin scattering [17, 22]. An efficient separation method is to perform a polarization filtering by subtracting the 90 position image from the 0 position image. We select to perform the polarization filtering with the Blue images in order to take advantage of the higher scattering on this band of the spectrum by both the epidermis and the dermis [15, 16]. The Blue0 image contains two components, the single scattered $Blue0^s$ and the multiple scattered $Blue0^m$, and the Blue90 only one, that of multiple scattering component and which is equal to the multiple scattering component of the Blue0 ($Blue0^m$ = Blue90). The result Scattering Contrast (Eq. (3)) is an image specific for the single scattered photons which originate from the epidermis or the very first layer of the dermis:

$$\textbf{Scattering Contrast} = Blue0 - Blue90 = Blue0^s + Blue0^m - Blue90 = Blue0^s \quad (3)$$

In the resulting image of Eq. (3), structures with high scattering properties appear bright, and structures with reduced scattering properties appear dark. By assigning the 255 grayscale value to the maximum value and the 0 grayscale value to the minimum, the contrast is maximized. Skin regions which pose 'normal' scattering properties usually occupy the

#175601 - $15.00 USD Received 14 Sep 2012; revised 10 Dec 2012; accepted 7 Jan 2013; published 20 Feb 2013

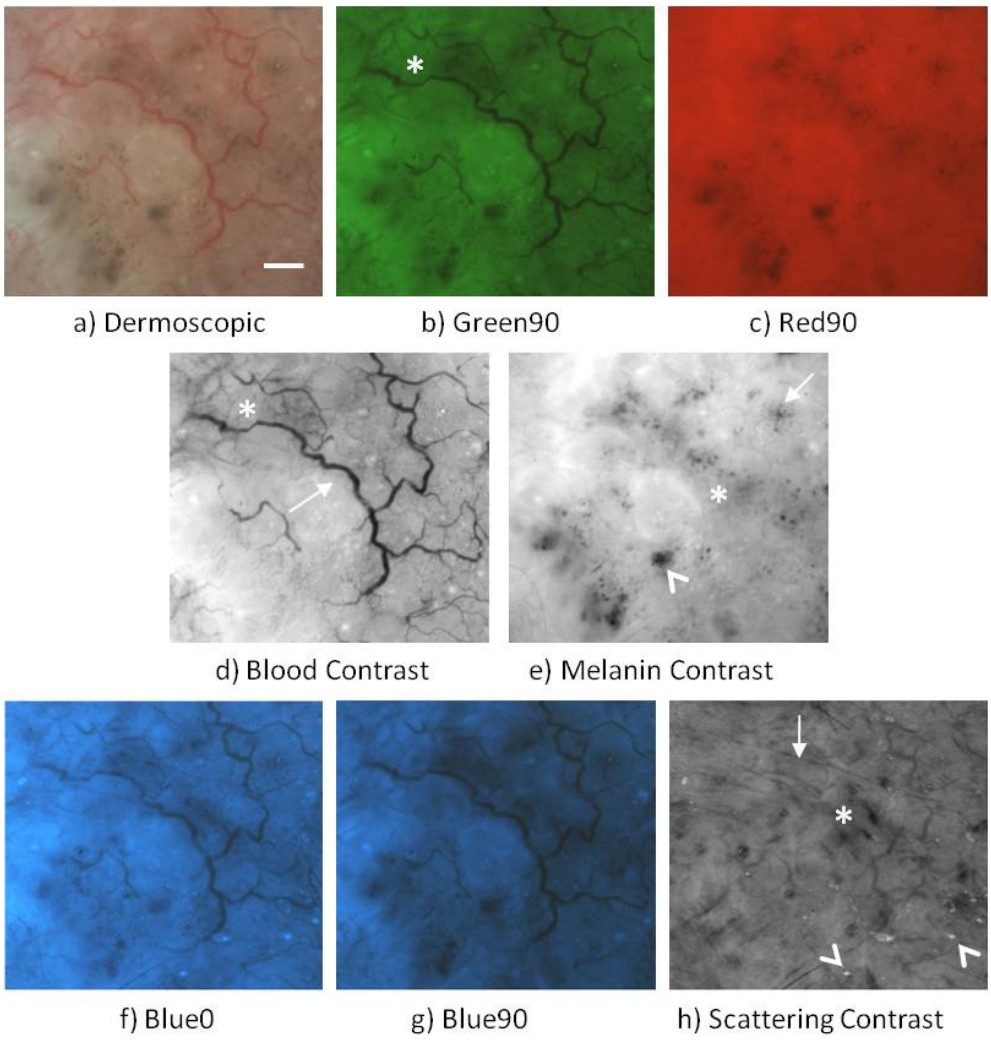

Fig. 2. A case of Basal Cell Carcinoma (BCC) a) Dermoscopic image (White90), scale bar: 1mm, b) Green90, star: small arborizing vessels, c) Red90, d) Blood Contrast, arrow: arborizing blood vessel, star: small arborizing vessels, e) Melanin Contrast, arrow: spoke wheel area, star: peppering morphology, arrowhead: large ovoid nest, f) Blue0, g) Blue90, h) Scattering Contrast, arrow: wrinkle, star: epidermal proliferation, arrowhead: Milia-like cysts (scale bar:1 mm).

majority of the imaged surface and have values in the middle of the 255 grayscale range. Therefore, the Scattering Contrast image is an image coding for scattering gradient.

In Fig. 2 the result of Scattering Contrast for a BCC case is illustrated. In Fig. 2(f) and Fig. 2(g) the Blue0 and Blue90 images are illustrated side by side. By visual inspection only, it is not possible to distinguish any differences. However, after the operation of Eq. (3), the resulting Scattering Contrast (Fig. 2(h)) image is very different compared to the blue images. Here contrast comes from single scattering and not from absorption, and several scattering structures are revealed. First, the surface texture of the lesion can be examined. Surface texture refers to the wrinkle network of the stratum corneum. In this case it appears stretched with only few big irregular wrinkles (arrow). Usually, in healthy skin, the wrinkle network is well structured and visible. This appearance in this lesion is an indirect indication that the morphology of the epidermis has altered; it has thickened, and this thickening has stretched

#175601 - $15.00 USD Received 14 Sep 2012; revised 10 Dec 2012; accepted 7 Jan 2013; published 20 Feb 2013

the surface of the lesion, and for this reason the normal wrinkles present before the lesion was created have disappeared. Instead, new, big, irregular wrinkles have been created.

Apart from the surface texture in this image, several dark structures appear inside the lesion. These structures appear dark, which means that they exhibit reduced scattering properties compared to adjacent skin regions. Also, they do not have well defined borders opposed to some superficial scattering structures which exhibit well defined borders, such as the wrinkles in Fig. 2(h) and Fig. 3(i). Such structures are not visible in classical dermoscopy and therefore histopathological examination is required to reveal their nature. However, we believe that such structures (star in Fig. 2(h)) are located not very close to the surface but rather in the base of the epidermis and may correspond to regions of epidermal proliferation inside the dermis. This morphology has also been visualized with our methodology in other cases of BCC (data not shown). If future histological examination revealed a correlation of this morphology to the underlying pathology those structures could be used as a diagnostic relevant feature.

Another scattering structure is observed on the lower right corner of Fig. 2(h) (arrowhead). Several bright spots appear which correspond to Milia-like cysts. Increased single scattering from these cysts results in bright spots in the Scattering contrast image. Milia-like cysts are well known structures which histologically correspond to intraepidermal keratin cysts and are usually found in cases of Seborrheic Keratosis, but can also be found, less frequently, in other types of lesions [3–5]. Many modern dermoscopes employ cross polarized illumination for enhancing the contrast of deeper structures of the skin. However, in such configurations, single scattering is eliminated and structures like Milia-like cysts appear with much less contrast or not at all [30]. With our methodology, such structures are imaged with higher contrast thus making their identification easier.

3.2 Melanocytic lesions

After a lesion is classified as melanocytic, a set of processing algorithms are applied to enhance the morphological features of the lesion. Because such lesions have a strong contribution from melanin, further processing steps have to be applied in order to remove or isolate this contribution. The algorithms applied are the Melanin Contrast, the Superficial Melanin Contrast, the Melanin Corrected Blood Contrast and the Scattering Contrast.

3.2.1 Melanin contrast

The aim of this processing method is to image the localization of melanin, and the result is divided in two images. One is the Melanin Contrast and the other is the Superficial Melanin Contrast. Melanin in melanocytic lesions can occupy large regions; it often proliferates inside the epidermis, and, in some cases, such as in melanoma, can escape to the dermis. Dermoscopic images are two dimensional images where any depth information is lost. In classical dermoscopy depth is sometimes estimated based on the hue of the color of melanin, assigning black for superficial melanin localization, and brown/dark brown for deeper localization. However, this is more similar to an empirical law. Here we develop a method for imaging melanin localization by producing two images; one for superficial melanin distribution and the other for deeper melanocytic structures.

The operations for the Melanin Contrast image are described in Eq. (1). Red light can, due to the reduced scattering and absorption, penetrate deeper inside the skin, and therefore can interrogate deep regions. Because absorption of melanin is significantly reduced in red compared to shorter wavelengths, superficial melanin concentration with small depth extension is almost invisible in the Red90 image. On the other hand, melanocytic structures which have a considerable size and have a certain depth extension are imaged with higher contrast in this image compared to the Blue90 and Green90 images. Therefore the Melanin Contrast result for melanocytic lesions is an image which is specific for relatively big and

#175601 - $15.00 USD Received 14 Sep 2012; revised 10 Dec 2012; accepted 7 Jan 2013; published 20 Feb 2013

deeper located melanocytic structures, and superficial melanocytic structures appear with reduced contrast.

The second part of our image analysis approach is to have an estimate for the more superficial localized melanin. The information on the superficially localized melanin is contained with much higher contrast in the Blue90 and Green90 images. Our strategy for extracting this information efficiently is to subtract the Green90 from the Blue90. By performing this subtraction, the effect of deeper localized melanin absorption (a morphology with low contrast in these images) is subtracted, but also the effect of hemoglobin absorption is subtracted. However, the effect of superficial melanin absorption is not completely subtracted, therefore the contrast in this new image is supplied by the difference in absorption of the more superficial melanin between blue and green spectrum. The difference of these images is divided with their sum for normalization. The Superficial Melanin Contrast (Eq. (4)) image is the image where the superficial localization of melanin can be visualized with higher contrast, and this image is free from hemoglobin absorption and deeper localized melanocytic structures. This result (Eq. (4)) is useful further in our analysis as it is going to be described below in the Blood contrast algorithm:

$$\text{Superficial Melanin Contrast} = \frac{\text{Blue90} - \text{Green90}}{\text{Blue90} + \text{Green90}} \tag{4}$$

When examining a lesion, the Melanin Contrast serves the purpose of identifying the relatively big and deep melanocytic structures that may exist in a lesion, and the Superficial Melanin Contrast image serves the purpose of imaging the distribution of melanin near the surface of the lesion. Finally, comparison of these two images provides a more complete view on the exact localization of melanin. Presence of melanin is encoded with darker gray values according to its relative concentration.

A case of a melanocytic lesion is illustrated in Fig. 3. In the dermoscopic image (Fig. 3(a)) a general view of the lesion is provided and the conventional dermoscopic analysis can be carried out. Melanin Contrast (Fig. 3(d)) is calculated by maximizing the dynamic range of the Red90 image (Fig. 3(e)). Some dark structures can be observed on the upper part of the lesion (arrow). They extend deep in the epidermis and they have irregular shape. On the Superficial Melanin Contrast result (Fig. 3(f)) the localization of melanin on the more superficial layers of skin can be seen. Here some globular structures (arrowhead) have higher contrast, and this is an indication that they are located near the skin surface and do not proliferate deep in the epidermis. Comparison of these two images (Fig. 3(e) and 3(f)) reveals that in the superficial layer of skin there is some diffuse melanin in the center of the lesion and some globular patterns in the periphery of the lesion (arrowhead). Some deeper localized structures appear in the center of the lesion (arrow), with irregular shape. One additional observation is that there is absence of a pigmented network, a morphology which is commonly seen in melanocytic lesions. The clinical diagnosis for this lesion was a melanocytic nevus.

3.2.2 Melanin corrected blood contrast

The aim of this processing algorithm is to increase the contrast for blood vessels. The additional complication in melanocytic lesions is the presence, in high concentration, of melanin which obscures the presence of blood vessels or completely masks it. Therefore, the target here is to create an image more specific for hemoglobin absorption. To achieve this, two processing steps are required. The first step is the same as followed for non-melanocytic lesions, and involves the subtraction of the Red90 image from the Green90 image and division with their sum. This operation is exactly the same as in Eq. (2). As mentioned above, the Red90 image has higher contrast for the deeper laying structures; therefore this operation only subtracts the contribution of deeper melanocytic structures and not superficial ones. As a

#175601 - $15.00 USD Received 14 Sep 2012; revised 10 Dec 2012; accepted 7 Jan 2013; published 20 Feb 2013

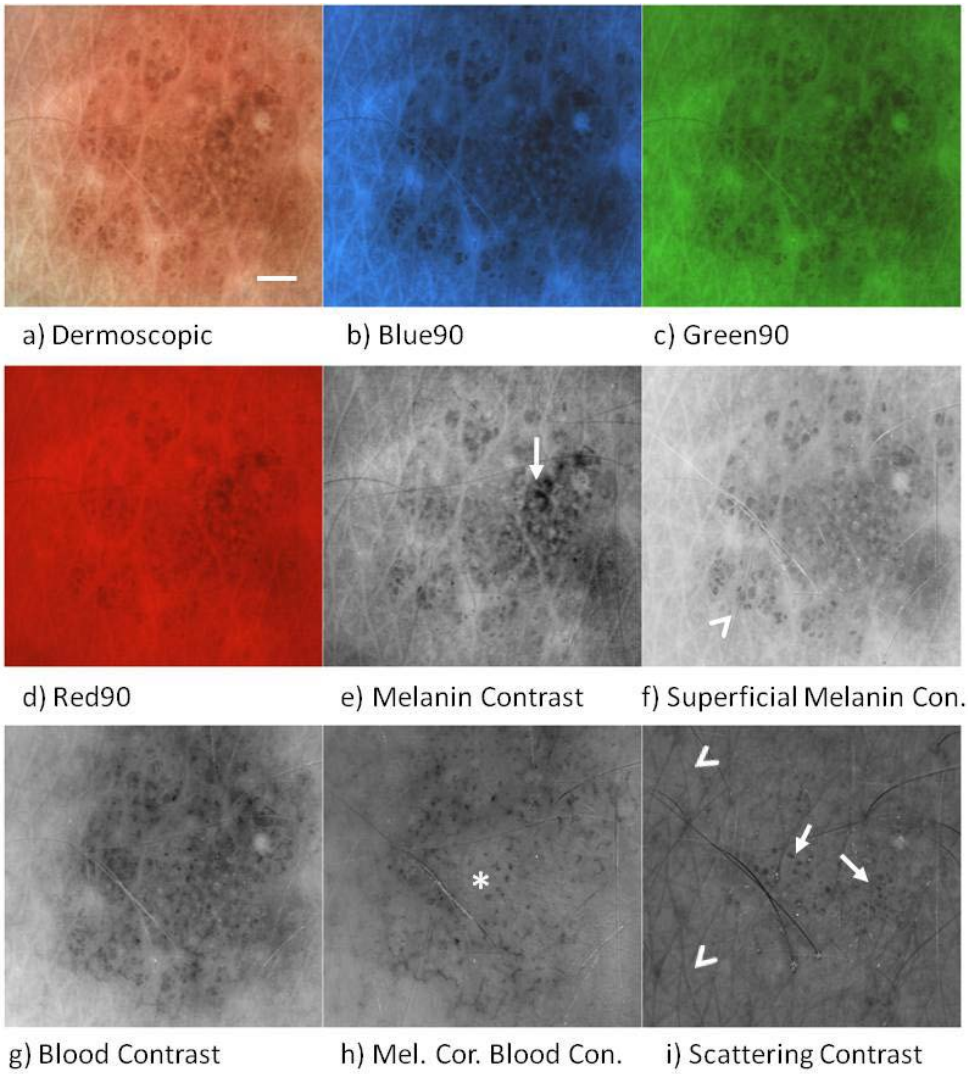

Fig. 3. A case of melanocytic mole a) Dermoscopic image, scale bar: 1mm, b) Blue90 image, c) Green90, d) Red90 image, e) Melanin contrast, arrow: deep melanocytic structures f) Superficial Melanin Contrast, arrowhead: superficial globular melanocytic structures g) Blood Contrast, h) Melanin Corrected Blood Contrast, star: dot vessels, i) Scattering Contrast, arrow: Comedo-like openings, arrowhead: wrinkles (scale bar:1 mm).

consequence, at this processing stage melanin subtraction is incomplete. In order to completely subtract the effect of melanin the superficial component has to be subtracted, and this information is contained in the Superficial Melanin Contrast result (Eq. (4)). The final Melanin Corrected Blood Contrast image is formed when the Superficial Melanin Contrastis subtracted from the Blood Contrast (Eq. (2)). The images used for the operation in Eq. (5) are 8-bit, and the resulting image is also converted in 8-bit in a similar manner as is done in Eq. (1). The resulting Melanin Corrected Blood Contrast image has high contrast for hemoglobin, and the absorption of melanin is cancelled out. In this image the vessel morphology can be observed with good detail:

Melanin Corrected Blood Contrast=Bloon Con.-Superficial Melanin Con. (5)

#175601 - $15.00 USD Received 14 Sep 2012; revised 10 Dec 2012; accepted 7 Jan 2013; published 20 Feb 2013

An example of the application of this algorithm on a melanocytic lesion is illustrated in Fig. 3(g) and 3(h). In the Green90 (Fig. 3(c)) image, as also in the dermoscopic image (Fig. 3(a)), blood vessels are not visible. Performing the first step of the processing algorithm reveals the blood vessels in the perilesional region, but also inside the lesion. However, presence of melanin absorption diminishes their contrast. The dermoscopic analysis is intended to be performed in the Blood Contrast image of Fig. 3(h) where the blood vessel morphology is revealed with high contrast and melanin contribution has been completely removed. In this image, the vasculature of this lesion can be observed, which otherwise would have been impossible in the dermoscopic image (Fig. 3(a)). Visual inspection of Fig. 3(h) reveals normal blood vessels in the periphery of the lesion and inside the lesion some dot vessels (star). Dot or dotted vessels are small vessels resembling the head of a pin and histologically correspond to vessels perpendicular to the skin surface. This type of morphology is not considered suspicious for a melanocytic lesions [31].

3.2.3 Scattering contrast

This algorithm is exactly the same as in Eq. (3) and the outcome has the same significance and interpretation. As in the case of non-melanocytic lesions, absorption effects are minimized, and single scattering is enhanced.

This algorithm is applied on the melanocytic lesion of Fig. 3. The Blue90 (Fig. 3(b)) image is subtracted from the Blue0 image to produce the Scattering Contrast image (Fig. 3(i)). The surface texture of the lesion is revealed in this image. The wrinkle network appears normal around the lesion, and inside the lesion it appears to be disrupted. Usually, this disruption is followed by an elevation of the epidermis which creates a new surface topography inside the lesion as new bigger wrinkle lines appear. Furthermore, some dark dots (arrow) appear inside the lesion. Inspection of Fig. 3(b) reveals that these dots do not correspond to absorbing structures but rather to regions where single scattering is reduced. These structures are known in dermoscopy as Comedo-like openings and histologically correspond to keratin containing openings. What is most important is that this morphology is more visible in this type of image (Fig. 3(i)) compared to the dermoscopic image (Fig. 3(a)).

4. Discussion

Dermoscopy is a non invasive *in vivo* method for the examination of skin lesions. The diagnosis is based on the presence or not of specific morphologies which are known to correlate with pathologic conditions [3–5]. However, the identification of these morphologies is performed by visual inspection, and as such it is a subjective and complex method. One of the reasons is that the contributions from the various skin components is encoded in one image and very often these contributions are superimposed making identification equivocal. In order to improve the capabilities of dermoscopy, we have developed a methodology where the contribution of the major skin components is isolated and presented on separate images with increased contrast.

The device developed for the present study is a dermoscope, therefore, all principles of dermoscopy are respected. Similar to classical dermoscopy, lesions are first classified as non-melanocytic or melanocytic, and different image analysis is followed for each case. The ABCD rule of dermoscopy and other pattern analysis methods can still be practiced. Up to this point, there is no difference between our approach and that of classical dermoscopy. However, further image processing by means of spectral and polarization filtering can provide additional information not obtainable with classical dermoscopy.

The distribution of melanin is illustrated in the Melanin Contrast image. For non-melanocytic lesions, small scale melanocytic structures are illustrated with high contrast on the Melanin Contrast result (Fig. 2(e)). For melanocytic lesions, visualization of the melanin distribution is divided in two images. On the Melanin Contrast image, the deeper melanocytic structures are visualized with high contrast, whereas the superficial distribution of melanin is

#175601 - $15.00 USD Received 14 Sep 2012; revised 10 Dec 2012; accepted 7 Jan 2013; published 20 Feb 2013

visualized with better contrast on the Superficial Melanin Contrast image (Fig. 3(f)). The study of the melanin distribution in a lesion is diagnostically important since specific morphologies have been found to correlate with specific pathologies [5]. The enhanced contrast of these structures in the Melanin Contrast image could make their identification easier.

The vasculature of a lesion is illustrated on the Blood Contrast image. Even though in non pigmented lesions imaging of the vasculature is also possible with conventional dermoscopy, with our methodology the Blood Contrast produces a high contrast image specific for blood vessels. Such an image provides a more detailed map of the vasculature. The presence of blood vessels in the papillary dermis is normal. However, in pathologic conditions specific vessel morphologies, such as the 'arborizing' morphology illustrated with high contrast in Fig. 2(d), have been found to correlate with malignancy [3–5, 31]. The major advantage of our methodology is in melanocytic lesions. As seen in the case of the melanocytic lesion (Fig. 3), the vasculature, which is not visible in the dermoscopic image (Fig. 3(a)), can be revealed in the Blood Contrast image (Fig. 3(h)). The examination and identification of the vessel morphology in an image which is free of melanin and specific for blood vessels is a less complex task.

Finally, the scattering potential of a lesion is illustrated on the Scattering Contrast. Numerous structures with distinct scattering properties can be found on skin lesions. Their contrast in common dermoscopic images is low, and therefore the study of some of these features, such as the surface texture, is new to dermoscopy. However, scattering structures exist, and they can be highlighted or even revealed in the Scattering Contrast result. The diagnostic relevance for some of these features has not yet been established clinically. However, the capability of enhancing the contrast for structures such as milia-like cysts (Fig. 2(h)) and comedo-like openings (Fig. 3(i)), which are structures already correlated with pathologic conditions, demonstrates the potential of the methodology developed, and it could be a promising new tool for dermoscopic analysis in the future. The objective of dermoscopy is the observation and identification of pathological morphologies. With our methodology we enhance the contrast of some specific morphologies therefore we always expect to observe them with much higher contrast compared to the classical dermoscopic images. The amount of contrast enhancement has to be evaluated in bigger scale clinical examination.

The instrument developed is practical, simple to use, and inexpensive. It records color images similar to existing digital dermoscopes. The selection of a RGB sensor instead of a monochrome sensor was made for compatibility reasons. On the current implementation acquisition of a dermoscopic equivalent image is straightforward. If a monochrome sensor was selected instead, then acquisition of color images would not be possible and reconstruction of color images from the spectral images would be necessary in order to create a dermoscopic equivalent image. The methodology described here was developed for RGB sensors, which is the type of sensors the majority of commercial dermoscope use. Therefore our methodology could be directly translated to existing dermoscopes with only minimal modifications. The required modifications would concern the illumination configuration and the polarization gating. Advances in LED technology have demonstrated the capability of constructing LED systems with several different wavelengths emitters on one chip. Use of such LEDs could reduce the size of the dermoscope head significantly. A miniaturized dermoscope head including the illumination set-up and the polarization optics could be directly adjusted on commercial dermoscope cameras. Therefore, our methodology could be directly transferred to the clinical practice without any sacrifices to the already established methods and advantages of classical dermoscopy.

5. Conclusion

The function and the results of the Polarization Multispectral Dermoscope have been demonstrated. This device can perform as a conventional dermoscope, but can also provide

#175601 - $15.00 USD Received 14 Sep 2012; revised 10 Dec 2012; accepted 7 Jan 2013; published 20 Feb 2013

additional morphological information about a skin lesion. Production of separate images specific for melanin, hemoglobin, and single scattering, increases the contrast for diagnostically relevant structures, and therefore could facilitate the diagnostic procedure, but also increase its specificity. Although these results are preliminary, and the sensitivity and specificity have yet to be evaluated on a bigger scale clinical examination, combination of classical dermoscopic analysis with our methodology could lead to a more accurate diagnosis.

Acknowledgments

The research leading to these results has received funding from the European Union Seventh Framework Programme (FP7/2007-2013) under grant agreements n° 228334 and n° 284464 (Bioptichal) and from the Italian Ministry for Education, University and Research in the framework of the Flagship Project NANOMAX. D. Kapsokalyvas gratefully acknowledges funding from the European Commission under the Marie Curie Host Fellowships Action for Early Stage Research Training ATLAS programme (MEST-CT-2004-008048). Financial support by the Ente Cassa di Risparmio di Firenze (private foundation) is acknowledged.

#175601 - $15.00 USD Received 14 Sep 2012; revised 10 Dec 2012; accepted 7 Jan 2013; published 20 Feb 2013